Deposition of Transparent and Conductive $In_4Sn_3O_{12}$ Using DC and HiPIMS Reactive Magnetron Sputtering

P. Butler, A. Cook, and H. Assender, Department of Material Science, University of Oxford, Oxford, United Kingdom;*
and P. Kelly, Surface Engineering Group, Manchester Metropolitan University, Manchester, United Kingdom

ABSTRACT

In this work, transparent conducting $In_4Sn_3O_{12}$ has been deposited onto 12 µm thick PET web and glass by means of reactive magnetron sputtering. The lower indium content required in the sputter target to produce this compound makes it attractive over conventional ITO. Previous work has demonstrated that this material can be produced with similar properties to industrial ITO (Minami, 1997, Thin solid Films Vol. 308 – 309). Both pulsed DC and HiPIMS power supplies have been utilised on an experimental deposition rig, and a semi industrial scale web coater. Films produced have been characterised in terms of their electrical, optical, chemical and physical properties. Resistivities in the region of $1x10^{-3}$ have been measured on polymer, with optical transparencies of 70 -80 % at thickness of 100 – 200 nm on glass. XRD analysis showed no dominant crystalline orientation, with AFM imaging also supporting the possibility of an amorphous film.

INTRODUCTION

There is a drive within the optoelectronics industry to replace certain glass components with flexible polymers due to the opportunity for low cost processing, mechanical flexibility, and lower weight. Plastic substrates may be produced and coated extremely rapidly in great volume. There are, however, a number of difficulties associated with the use of polymer substrates; the most important being reduced working temperature, greater roughness and coating damage during handling. Our roll-to-roll web vacuum coating facility allows deposition of both organic and inorganic layers, such as might be used to manufacture flexible display, OFET and PV materials. This work involves deposition of one important component of many devices, the transparent electrode material, onto polymer web in a roll-to-roll environment. Conventional DC magnetron sputtering is a mature technology, and has been used to successfully deposit TCO films onto a range of substrates. HiPIMS is a relatively new form of sputtering, which has promised a number of advantages over other forms of sputtering for certain applications. In particular for this application the prospect of low heat load on the substrate during deposition and the possibility to create more dense, ordered coatings without use of substrate heating, makes HiPIMS a particularly attractive prospect.

The ternary oxide $In_4Sn_3O_{12}$ is often formed in small quantities when depositing traditional ITO, but has received relatively little attention as a TCO in its own right. A major benefit of sputtering this oxide as opposed to the more common doped indium oxide is that indium content in the sputter target may be reduced by 45 % or more. This represents a significant reduction in cost and also reduces the demand for Indium, which is a rare element. Previous work has concentrated on the deposition of $In_4Sn_3O_{12}$ onto inflexible substrates, in which films of properties similar to that of traditional ITO shown to be possible [1, 2]. This work will demonstrate that $In_4Sn_3O_{12}$ can be deposited onto unheated glass and PET substrates in a rotational environment to produce conducting and transparent films with resistivities of ~ $1x10^{-3}$ Ω cm and an average transparency in the visible region of 70 % on glass at a thickness of ~150 nm.

It is well known that indium oxide thin films usually grow with a strong columnar c-axis oriented structure. In a typical polycrystalline film such as ITO, grain boundary scattering as well as the mechanisms found in single crystal materials will limit charge mobility, and hence conductivity. The limited temperature window in which PET can be processed limits any post-deposition annealing, and also the sputter power that can be used in conventional DC sputtering. It is interesting to note that whilst AZO films produced using our DC sputter cathode show a strong preferred crystalline orientation, $In_4Sn_3O_{12}$ films produced under similar conditions appear amorphous under XRD analysis, regardless of thickness. Other authors have shown $In_4Sn_3O_{12}$ to have a strong preferred crystalline orientation similar to that of ITO [1, 3]. One explanation for this could be a lack of sufficient energy of the sputtered species arriving at the growth surface to reorganise to form a preferred orientation. HiPIMS has been shown to minimise substrate heating whilst maximising ionisation of sputtered species, and thus is particularly suited to polymer substrates where a dense crystalline film is required. It is hoped that the highly energetic species that result from the HiPIMS discharge might also give rise to superior film properties, whilst maintaining a low substrate temperature. Initial results have proved promising, however work is continuing to more thoroughly characterise the films produced using HiPIMS. This work will seek to compare DC with HiPIMS deposition in a roll-to-roll context.

**SVC Sponsored Student*

 505/856-7188
54th Annual Technical Conference Proceedings, Chicago, IL April 16–21, 2011 ISSN 0737-5921

EXPERIMENTAL PROCEDURE

Early stage, small scale deposition was carried out in a modified Edwards 306 coating unit. A single 3" diameter circular magnetron supplied by Moorfield was enclosed by a bespoke shield, and substrates were mounted to a rotatable aluminium cylinder. This allowed simulation of our full scale roll-to-roll webcoater, although full web handling capability was not available on the small scale equipment. The metallic targets were indirectly water cooled, and clamped to the surface of the magnetron without need for a backing plate. DC powers of up to 1 kW were possible, although no specification for use with HiPIMS is available for this particular cathode. Glass and / or silicon slides could be coated simultaneously to the polymer web to allow for certain materials characterisation that would prove difficult on PET. Sputter and reactive gas was controlled by means of up to four Advanced Energy mass flow controllers, with control possible to 0.01sccm.

The industrial scale roll-to-roll coater was supplied by Aerre of Italy, and has a web handling capability of up to 8 km at 350 mm width. Web speeds of 300 m/minute are possible, but the coater will run as slow as 1 m/minute if required. The coating chamber is fitted with twin rectangular sputter cathodes, capable of handling 10 kW. Web drive and gas flow is handled via a bespoke computer interface. Whilst gas flow is only controllable to 1 sccm, more accurate control can be achieved by use of the more precise MFCs from the small scale equipment.

Direct current power was provided by a 12 kW Advanced Energy MDX unit, coupled to an Advanced Energy sparcLE arc suppression module. Both Hüttinger and Melec HiPIMS supplies were utilised during this work.

Process parameters investigated were: chamber pressure, deposition power and oxygen flow rate. Electrical conductivity was measured by a Jandel linear four point probe. Carrier concentration and mobility were measured via an Ecopia HMS-3000 Hall Effect system. Optical transparency and absorption was measured on samples deposited on glass over wavelength range 400-800 nm on a Varian Cary 5000 UV-Vis-NIR spectrometer. Film thickness was measured on a Veeco Dektak 6M stylus profiler, and topographical images produced with a Park Autoprobe CP atomic force microscope (AFM). Crystallographic information was taken using X-ray diffraction (XRD).

RESULTS AND DISCUSSION FOR DC SPUTTERING

Small Scale Apparatus: Effect of Sputter Discharge Power

$In_4Sn_3O_{12}$ films were deposited on glass and PET web via the rotating substrate drum at 0.85A, 1.35A and 1.85A in current control mode. Increasing current corresponds to a higher discharge power. If a simplified view of the plasma sheath is taken, these currents correspond to a power density on the cathode surface of 5.4 W cm^{-2}, 10.8 W cm^{-2}, and 16.2 W cm^{-2} respectively. This simplification also ignores any effect of target erosion on the surface area, but will serve as a reference with which to compare results on the web coater.

Table 1 gives values for resistivity, transparency (on glass), band gap, carrier mobility and concentration, and deposition rate for the most conductive sample (i.e. that with an optimised oxygen flow rate) produced at each of the three currents under investigation. Where possible, data have been averaged over the central homogeneous region of the sample. Chamber pressure was maintained at $4x10^{-3}$ mbar, with the partial pressures of argon and oxygen varied to investigate different stoichiometries. Deposition time was varied to ensure all films were approximately 150nm in thickness.

Table 1: Properties of most conductive films produced at 0.85A, 1.35A and 1.85A.

Discharge current	0.85A	1.35A	1.85A
Resistivity (Ω cm)	$2.35x10^{-02}$	$5.17x10^{-03}$	$8.91x10^{-04}$
Transparency %	76.1	79.4	80.5
Band gap (eV)	4.16	4.14	4.15
Carrier concentration (cm^{-3})	-1.96E+19	-8.12E+19	-1.82E+20
Carrier mobility ($cm^2\ V^{-1}\ s^{-1}$)	5.5	19.2	23.3
Deposition rate (nm min^{-1})	9.7	21.3	30.0

As can be seen from the data, increased discharge power lead to improvement in general film properties. A full discussion of all films produced is not given here, but the general trends observed were that increasing mobility and carrier concentration could be achieved at higher discharge powers, after optimisation of oxygen flow. This enables more conductive films to be produced at higher powers. The deposition rate also increased as expected at higher powers. The material has a wide bandgap of around 4.15 eV, calculated by plotting the square of the absorption coefficient multiplied by the photon energy $(\alpha.h\nu)^2$ against photon energy $h\nu$ [4,5]. Transparency showed an increase with increasing discharge power, but was highly dependent on oxygen flow

XRD analysis of the films showed no evidence of crystallinity. AFM imaging of the sample surface revealed randomly ordered spherical grains as shown in Figure 1. Interestingly, the average diameter of these grains did not show an increase with increased discharge power. This is contrary to the outcome one would expect when imaging a crystalline film,

such as the aluminium doped zinc oxide (AZO) films also shown in Figure 1 for reference. The strongly c-axis oriented AZO shows a marked increase in crystallite diameter as the discharge power is increased from 0.85A to 1.85A, whereas the indium tin films show no such increase. Both materials were produced under similar conditions.

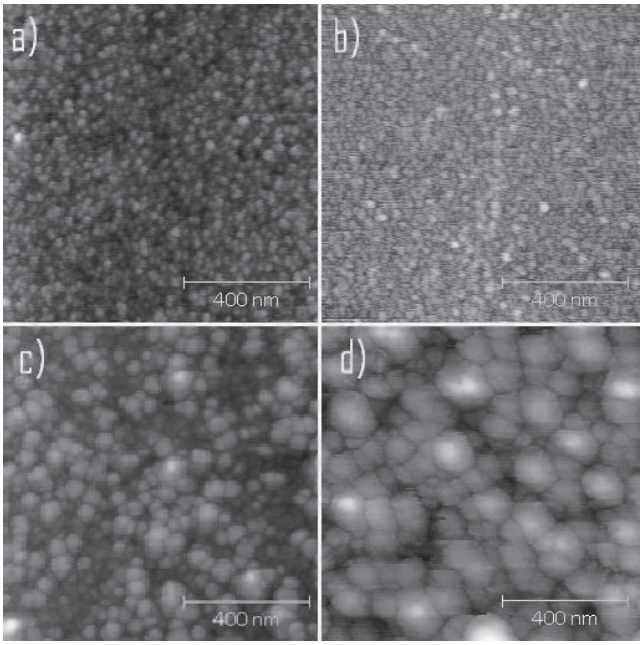

Figure 1: AFM topographical images a) indium tin at 0.85A, b) indium tin at 1.85A, c) AZO at 0.85A, d) AZO 1.85A.

Small Scale Apparatus: Effect of Chamber Pressure

The effect of chamber pressure on conductivity and transparency was examined by depositing a set of films at $1x10^{-3}$ mbar, $2x10^{-3}$ mbar and $4x10^{-3}$ mbar. A fixed sputter current of 1.35A was used, with chamber pressure regulated by throttling the diffusion pump. The resulting film characteristics have been summarised in Figure 2.

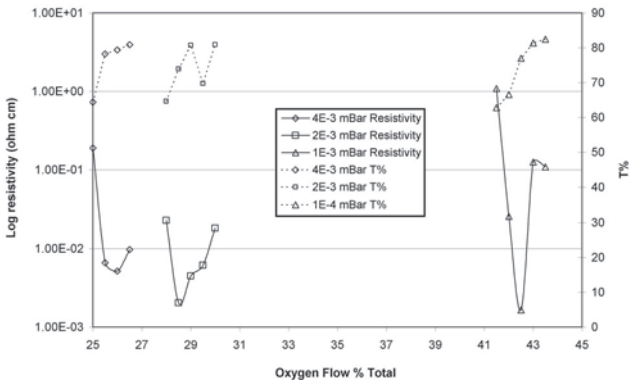

Figure 2: Chart showing average resistivity and average optical transmission of indium tin films deposited at $1x10^{-3}$, $2x10^{-3}$ and $4x10^{-3}$ mbar at 1.35A as a function of the reactive gas flow.

As the chamber pressure is reduced, so too does the minimum resistivity possible. There is also a small but noticeable increase in the maximum optical transmission. Reducing the chamber pressure also appears to make the resulting film properties increasingly sensitive to oxygen flow, with a narrower process window available for highly conductive films at lower chamber pressures. Both the carrier concentration and mobility increased in films made at lower pressure. A general trend is observed that as the oxygen level is increased, carrier concentration reaches a maximum coinciding with minimum resistivity, before falling again at higher oxygen flows. Mobility is seen to increase with oxygen level. Table 2 gives values for resistivity, transparency, band gap, carrier mobility and concentration, and deposition rate for the most conductive sample produced at each of the three pressures under investigation.

Table 2: Properties of most conductive films produced at $1x10^{-3}$, $2x10^{-3}$, and $4x10^{-3}$ mbar.

Chamber pressure	$1x10^{-3}$ mbar	$2x10^{-3}$ mbar	$4x10^{-3}$ mbar
Resistivity (Ω cm)	$1.65x10^{-3}$	$2.05x10^{-3}$	$5.17x10^{-3}$
Transparency %	77.0	80.7	79.4
Band gap (eV)	4.15	4.15	4.14
Carrier concentration (cm^{-3})	-1.80E+20	-8.93+19	-8.12E+19
Carrier mobility ($cm^2 V^{-1}s^{-1}$)	23.3	20.4	19.2
Deposition rate (nm min^{-1})	20.0	24.8	21.3

Large scale deposition of $In_4Sn_3O_{12}$

Initial results using the large scale roll-to-roll webcoater have indicated that it may well be possible to produce films with good properties on full scale industrial equipment. Difficulty was encountered however with target damage due to excess heat build-up on the surface; the melting point of this composition, close to the eutectic indium – tin (1:1) alloy being 120°C [6]. Because of the low melting point of the target, the work was limited to low power densities. Improved target cooling would of course allow for higher power densities to be utilised.

Because of the lengthy pumping times required to achieve satisfactory vacuum levels (~$6x10^{-5}$ mbar before argon backfilling), multiple films were produced on static glass and PET substrates mounted around the coating drum. This allowed for up to four samples to be deposited with no need to vent and re-evacuate between depositions. Films produced were sufficiently homogeneous across the region of interest to allow for meaningful analysis, due to the size of the cathode far exceeding the size of the sample.

Films were produced at sputter currents of 2.85A and 3.35A. This corresponds to a power density at the cathode, ignoring the effect of target erosion, of 2.7 W cm^{-2} and 3.3 W cm^{-2} respectively – note this is lower than the power densities used on the small scale equipment. Both currents produced transparent and conductive films when sputtered with the correct flow of oxygen present in the chamber. From the limited number of samples available, it is not possible to conclude that the higher current would produce more conductive films (although it is highly likely), however it is possible to say that the process window for good film properties was wider at 3.35A than at 2.85A. Figure 3 shows the resistivity and transparency of films produced at 3.35A.

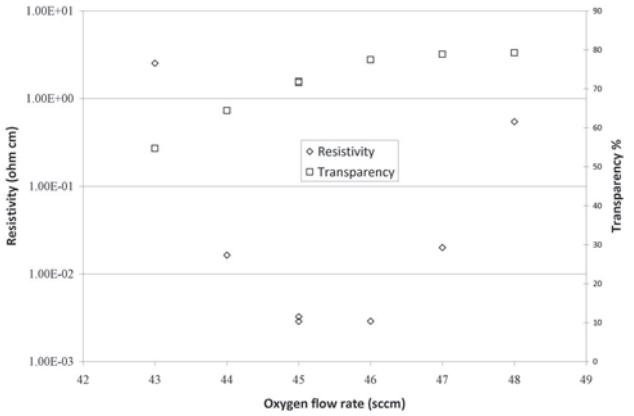

Figure 3: Graph of resistivity and average transparency of films produced on the webcoater at 3.35A as a function of oxygen flow rate.

As with the small scale films, a trend of increasing transparency is observed as the oxygen flow rate is increased, and the resistivity passes through a minimum before climbing again as the films become more stoichiometric. The deposition rate was dependent on oxygen flow, with values of 1.52 nm sec^{-1} at 43 sccm to 1.14 nm sec^{-1} at 48 sccm. A deposition rate of 1.31 nm sec^{-1} was achieved at 46 sccm, where film properties seem optimised at $2.9x10^{-3}$ Ω cm and 78.8% transparency (on glass). Rates were lower for samples produced at 2.85A.

Deposition of $In_4Sn_3O_{12}$ on a rotating drum is still being trialled, however early (non-optimised) films have yielded encouraging results. At a web speed of 1 m min^{-1} and a current of 3.35A, a transparent film of approximately 100nm thickness (with five passes of the cathode) has been deposited with resistivity of $4.7x10^{-2}$ Ω cm.

HiPIMS deposition of $In_4Sn_3O_{12}$

$In_4Sn_3O_{12}$ has been deposited on the small scale apparatus using both Hüttinger and Melec power supplies. It was noted that severe damage to the target was caused by arc events when the discharge entered the unstable poisoned region. Irregularities on the target surface also acted as centres for arcing, and lead to target failure due to a high concentration of arcing in a confined area. This phenomenon was seen with average powers at, and below those used on identical targets running DC power. Great care therefore had to be taken when introducing oxygen to the system to avoid entering the poisoned region, even briefly.

A single transparent and conductive sample was produced on the Hüttinger power supply as a trial to confirm HiPIMS could be used to deposit a film. The film was deposited at an average power of ~400W, a pulse-on time of 150 µs and a frequency of 200 Hz. A minimum resistivity of $2.25x10^{-3}$ Ω cm was recorded at a thickness of approximately 100 nm, although the properties showed large spatial variance across the width of the film, with a maximum resistivity of $5.31x10^{-2}$ Ω cm. Whilst some spatial variation is seen on films produced with DC, such a large variation of resistivity is unusual. As well as variations in properties from the central region to the edge of the sample (which are also observed in DC), a large variance was seen from left to right. This was attributed to uneven reactive gas coverage in the sputter region, due to the asymmetric design of the cathode shield and drum. In an effort to reduce this effect, subsequent depositions using the Melec supply were carried out with gas flow introduced outside of the cathode shield.

Three conductive and transparent films were produced with the Melec power supply. Extremely fine control of oxygen flow was required to maintain a stable sputter voltage in the region where the desired film properties could be achieved. A pulse-on time of 50 µs was selected, with a frequency of 995 Hz. The discharge power was fixed at 250W. Peak currents of ~180A were observed. Figure 4 shows the resistivities of the three films plotted against their position across the width of the slide, to illustrate the large variance in properties observed.

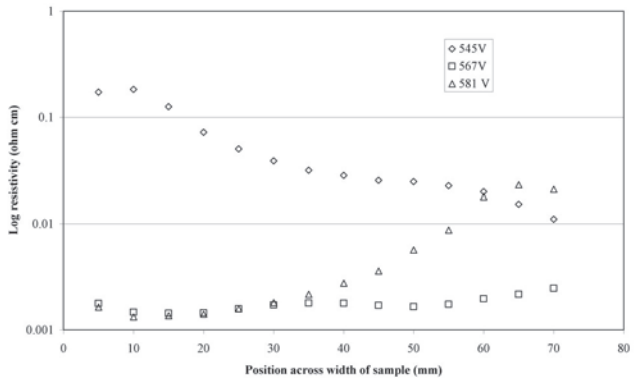

Figure 4: Graph showing resistivity of samples grown at 545V, 567V and 581V as a function of their position across the width of the substrate.

The film grown at 567V shows a more homogeneous spread of properties than those grown at 545V and 581V. This sample also exhibits consistently low resistivites. One would expect a

more homogeneous film when chamber conditions are close to the optimum state, as illustrated by Figure 3; where the trend for resistivity shows a steady state at 45 and 46 sccm, but a sharp increase in resistivity outside of that stable region. It is also notable that lower resistivities for the samples grown at 545V and 581V occur at opposite sides of the sample from one another, ie 545V exhibits lower resistivites on the left hand side and 581V on the right.

Carrier concentrations of $1.9x10^{20}$ cm^{-3} were observed, together with mobilities of 24 cm^2 $V^{-1}s^{-1}$ on both the 567V and 581V sample, although the concentration and mobility fell to $5.4x10^{19}$ cm^{-3} and 2.7 cm^2 $V^{-1}s^{-1}$ respectively at the right hand side of the 581V film. The low mobility would indicate that in this region the film is oxygen deficient. It would seem to be the case then that when oxygen flow is insufficient (voltage too high) to achieve optimum properties, the left hand side of the chamber has a slightly greater amount of oxygen available at the growth surface and thus exhibits *better* resistivities as shown by 581V. When the oxygen level is too great (voltage too low), the left hand side produces *poor* resistivities, shown by 545V.

A minimum resistivity of $1.3x19^{-3}$ Ω cm was recorded. This is comparable, if not slightly better than the resistivities seen when depositing at a similar power with DC. There is however insufficient data to conclude whether HiPIMS will produce better TCOs. Film thicknesses of 180 – 200 nm were measured at the centre of the two more conductive films (567 and 581V). This gives a deposition rate of 22.5 – 25.0 nm min^{-1}, which is again comparable to that of DC.

Optically, films showed the typical trend, with increasing oxygen flow (or in this case discharge voltage) leading to increased transparency. In the central area of each film (ie 30 – 40 mm) transparencies of 80.7 %, 67.2 % ,and 57.3 %were observed for 545V, 567V, and 581V respectively. A band gap of 4.1 eV was calculated for the films grown at 567V and 581V, and a band gap of 4.0 eV for the film grow at 545V.

From these preliminary results detailed here, it can be seen that HiPIMS produces films of comparable properties, but is more sensitive to oxygen flow rate than DC when depositing this particular material. It also highlights the need for good cathode design to ensure a homogeneous availability of oxygen at the growth surface. We have not yet had the opportunity to optimise the HiPIMS parameters for best film properties.

CONCLUSIONS

It has been show that $In_4Sn_3O_{12}$ may be deposited onto polymer web and glass slides using both DC and HIPIMS magnetron sputtering. Resistivities in the region of $1x10^{-3}$ Ω cm have been recorded, together with good (>70 %) transparency. To date, DC deposition has produced amorphous films that exhibit improved properties with increasing discharge power and decreasing chamber pressure. It has been possible to deposit $In_4Sn_3O_{12}$ using a large scale webcoater on a moving polymer web.

HiPIMS has been used to deposit $In_4Sn_3O_{12}$ films with properties comparable to those deposited by DC. It has proved more difficult however to achieve homogeneous films, due to the sensitivity of HiPIMS to the local oxygen level at the growth surface. More work to characterise the films produced will be performed to ascertain the differences between HiPIMS and DC, and this will hopefully lead to a conclusion as to which technique is better suited to depositing high quality TCOs onto polymer.

REFERENCES

1. Minami T, Takeda Y, Takata S, Kakumu T. Preparation of transparent conducting $In_4Sn_3O_{12}$ thin films by DC magnetron sputtering. Thin Solid Films 1997 10/31;308-309:13-8.

2. Minami T. Substitution of transparent conducting oxide thin films for indium tin oxide transparent electrode applications. Thin Solid Films 2008 2/15;516(7):1314-21.

3. O'Neil DH, Walsh A, Jacobs RMJ, Kuznetsov VL, Egdell RG, Edwards PP. Experimental and density-functional study of the electronic structure of $In_4Sn_3O_{12}$. Phys.Rev.B 2010 Feb;81(8):085110.

4. Pierson JF, Wiederkehr D, Billard A. Reactive magnetron sputtering of copper, silver, and gold. Thin Solid Films 2005 5/1;478(1-2):196-205.

5. Li H, Zhang Q, Pan A, Wang Y, Zou B, Fan HJ. Single-crystalline $Cu_4Bi_4S_9$ nano ribbons: Facile synthesis, growth mechanism, and surface photovoltaic properties. Chemistry of Materials 0;0(0).

6. Okamoto H. In–Sn (indium-tin). Journal of Phase Equilibria and Diffusion 2006;27(3):313.